IRAQI Academic Scientific Journals

Tikrit Journal of Engineering Sciences (2019) 26 (2) 9-14

ISSN: 1813-162X (Print) ; 2312-7589 (Online)

Tikrit Journal of Engineering Sciences

available online at: http://www.tj-es.com

TJES Tikrit Journal of Engineering Sciences

College of Engineering

Weis MM. The Performance Prediction of The Mixed Convection In an Inclined Circular Tube Filled Porous Media Based on an Intelligent Control. *Tikrit Journal of Engineering Sciences* 2019; **26**(2): 9-14.

The Performance Prediction of The Mixed Convection In an Inclined Circular Tube Filled Porous Media Based on an Intelligent Control

Musa Mustafa Weis*

Fuel and Energy Department
Technical College
Northern Technical University
Kirkuk
Iraq

***Keywords*:**

Mixed convection
porous media
inclined circular tube
artificial neural network thermal performance

ARTICLE INFO

Article history:

Received 07 Jan. 2019
Accepted 05 Apr. 2019
Available online 10 May 2019

ABSTRACT

The porous media has a significant impact on the heat transfer and storage properties. The present study focuses on the heat transfer of the mixed convection through a circular tube that filled with a porous media at different angles using a neural network. An experiment had been performed for the Rayleigh number range from 108.54 to 907.73 and the Peclet number range 30.3.-510 using three tests for the heat flux. The result shows the mean relative error about 7.913% and the coloration coefficient (R^2) Is 99.18% for the train data. The mean relative error about 6.641% and the R^2 is 99.46%, for the test data. The results showed that effectiveness of ANN in the predicted thermal performance in thermal engineering applications such as heat transfer modeling using porous media with airflow.

DOI: http://dx.doi.org/10.25130/tjes.26.2.02

تنبؤ آداء الحمل المختلط في انبوب دائري مائل مملوء بوسط مسامي قائم على تحكم ذكي وبيانات مختبرية

موسى مصطفى ويس قسم الوقود والطاقة/ الكلية التقنية/ الجامعة التقنية الشمالية / كركوك / العراق

الخلاصة :

الاوساط المسامية لها تأثير كبير على نقل الحرارة وخصائص التخزين. تركز الدراسة الحالية على انتقال الحرارة بالحمل المختلط عبر أنبوب دائري مملوء بالوسائط المسامية بزوايا مختلفة وذلك باستخدام شبكة عصبية. استخدمت البيانات الحقيقية في النتائج التجريبية. تم إجراء هذه التجارب لمجموعة أرقام رايلي ضمن المدى من 108.54 إلى 907.73 و رقم بكلت من 30.3 الى 510 وباستخدام ثلاثة اختبارات للفيض الحراري. اظهرت النتائج بان معدل الخطأ النسبي كانت حوالي 7.913٪ ومعامل التلوين كانت (R^2) 99.18٪ لبيانات التدريب. اما الخطأ النسبي قدر بحوالي 6.641 ٪ و(R^2)99.46 ٪ لبيانات الاختبار. حيث أظهرت النتائج فعالية ANN في التنبؤ بالأداء الحراري في تطبيقات الهندسة الحرارية مثل نمذجة نقل الحرارة باستخدام الوسائط المسامية مع تدفق الهواء.

الكلمات الدالة: الحمل المختلط، وسط مسامي، انبوب دائري مائل، شبكة اعصاب الصناعية، الاداء الحراري

* E-mail : musa.weis@ntu.edu.iq

Nomenclature

A_s Surface area (m^2)
c_{P_f} Specific heat of the air (J/kg K)
D Outside diameter (m)
d_p Grain diameter (m)
g Gravity acceleration (9.81 m/s^2)
Gr_z Grashof number
h_z Local convection heat transfer (W/m^{2o}C)
I current (A)
K permeability (m^2)
k_f thermal conductivity (W/m ^{o}C)
l tube length (m)
$\dot{m}$ mass flow rate (kg/s)
Nu_z Nusselt number
Pe Peclet number
Ra Rayleigh number
Re Reynolds number
Q power input (W)
q Heat Transfer rate (W)
q_w Heat flux (W/m^2)
T_{in} inlet temperature (^{o}C)
T_{out} outlet temperature (^{o}C)
u air velocity (m/s)
V supplied Voltage (V)

Greek symbols

ε Porosity
μ_f dynamic viscosity (N/m.s) or pas.sec
ρ_f density (kg/m^3)

1.Introduction

Researches had been directed in the last three centuries, especially after the increase of the demand for the energy in the world to attract work in two these areas are firstly looking for new alternatives to fossil energy, such as renewable energy and environment-friends. Second, to rationalize energy consumption by improving the performance of the thermal systems by looking for catalysts that lead to increase the heat transfer of these systems, such as the porous media in both types of a stuffed layer and fluidized bed [1-4]. Pu et al. [5].Experiments were conducted on two regimes of convection heat transfer (laminar and turbulent) in a vertical channel with non-uniform heating of the two opposite walls and working conditions in the range of 700<*Ra*< 1500 and 2<*Pe*< 2200 and the measured temperature distribution in the vertical packed channel indicates a secondary thermal cell within it. The correlation relation for the Nusselt number was obtained in terms of the number of Peclet and Rayleigh of the experimental data and plot their relationship. Three convection regimes have been noticed; forced convection $Ra/Pe < 1$, mixed convection $1 < Ra/Pe < 105$and natural convection$105 < Ra/Pe$. Many researchers study the mixed convection numerically [6-8], and experimental [9,10]

In many engineering applications, the artificial meshs had been used as it offer better and more logical solutions [11]. A feed-forward back propagation ANN was used to analyse in both numerical and experimental studies of heat transfers in the two-phases change process in an around the finned pipe. The average relative error in the experiment was about 5.58% while the numerical model ended with 14.99%.Fadare and Fatona [12] studied ANN in four kinds of exchanger models such as staggered multi-row, multi-column, cross-flow, and tube to a tube, the results were compared with the experimental data. Results showed that the relative error was less than 4% and 1% for testing and training data. Islamoglu and Kurt [13] used the ANN model to analyse the heat transfer rate of the corrugated channel. Results showed that the relative error between experimental and ANN results was less than 4%.

This study focused on the capability of ANN for heat transfer analysis in the circular tube filled with porous media horizontal and inclined with different angles as well as change the heat flux.

3.Experimental Setup

Experiments on convective heat transfer were carried out using the rig as shown in Fig.1, which consists of a circular copper tube of 45 and 47 mm inner and outer diameter respectively, 850mm length, it was filled with porous media and tube surface heated with a constant heat flux at different positions of the tube, starting from the horizontal and changing the angle to have different values 30^o, 45^o, 60^o, respectively. The heated tube length about 800 mm and it was packed with glass balls of 5mm diameter of thermal conductivity of 0.81W/m^{o}C. 48 thermocouples type T were used to measure temperature in the test tube. These thermocouples are fixed as; two thermocouples are allocated to measure the air inlet temperature and output and the rest were fixed with three thermocouples groups for each location in the tube. The outer surface of the tube is heated electrically using a 28-m of 0.1 Ω electrical resistance turns around the tube; voltage regulator was used as a power supply to the test heated tube section. The AM4200 anemometer was used to measure the air velocity. Figure 1 illustrates the schematic diagram of the experimental setup. (For more information about the experimental setup, please see Ref. [8]) .

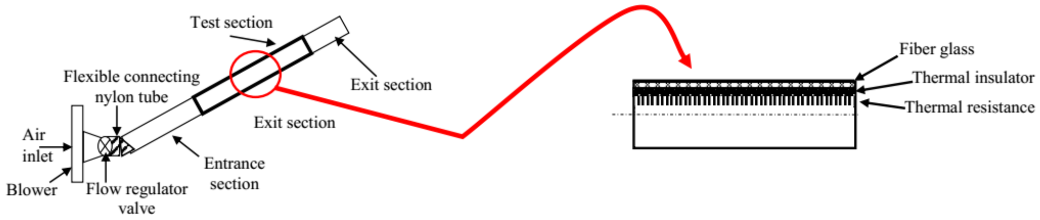

Fig.1. Schematics drawing of the experiment setup [14].

2.Data reduction

In the current experiment, the steady state is assumed. The air properties are evaluated using the following relations that based on the temperature range.$250\text{K} \leq 0.5(\overline{T_{in}} + \overline{T_{out}}) \leq 375\text{K}$[15].

$$\left.\begin{aligned} \rho_f &= 2.209 - 3.414\times10^{-3}\left(\frac{T_{in}+T_{out}}{2}\right), & \text{kg/m}^3\\ c_{P_f} &= \left[9.848 + 6.76\times10^{-4}\left(\frac{T_{in}+T_{out}}{2}\right)\right]\times10^{2}, & \text{J/(kg K)}\\ k_f &= \left[3.479 + 7.58\times10^{-2}\left(\frac{T_{in}+T_{out}}{2}\right)\right]\times10^{-3}, & \text{W/(m K)}\\ \mu_f &= \left[4.475 + 4.564\times10^{-2}\left(\frac{T_{in}+T_{out}}{2}\right)\right]\times10^{-6}, & \text{kg/(m s)} \end{aligned}\right\} \quad (1)$$

The porosity was taken about 0.3661, due to the absence of the regular arrangement of the porous media inside the tube compared with the calculated value using the Eq. (2) [2].

$$\varepsilon = 0.32 + \left[0.45\times\left(\frac{d_p}{d}\right)\right] \quad (2)$$

The value from Eq. (1) about 0.37. Therefore, the permeability could be found using Eq. (3) [17]:

$$K = \frac{\varepsilon^3 d_p^2}{175\times(1-\varepsilon)^2} \quad (3)$$

The local heat transfer coefficient could be evaluated as, follow:

$$h_z = \frac{q}{\left[T_s - \left(\frac{T_{in}+T_{out}}{2}\right)\right]_z} \quad (4)$$

and

$$q_w = \frac{q}{A_s} \quad (5)$$

where

$$A_s = \pi d l$$

$$q = \dot{m} C_{p,a}(T_{out} - T_{in}) \quad (5)$$

where the heat energy could be evaluated using the electrical power equation.

$$Q = I\times V \quad (6)$$

The efficiency of the converted electrical power could be calculated for the heat transfer rate as follow:

$$\zeta = \left(1 - \frac{q}{Q}\right)\times 100 \quad (7)$$

The local Nusselt number is defined as:

$$Nu_z = \frac{h_z d}{k_{eff}} \quad (8)$$

where k_{eff} is the effective porous media thermal conductivity which was determined as [18]:

$$k_{eff} = \varepsilon k_f - (1-\varepsilon)k_p \quad (9)$$

where $k_f$and $k_p$are the fluid and porous media thermal conductivity, respectively. Reynolds number was defined as [2]:

$$Re = \frac{\rho_f\, u\, d_p}{\mu_f(1-\varepsilon)} \quad (10)$$

Peclet number is defined as:

$$Pe = Re\, Pr_f \quad (11)$$

Grashof number (Gr) and Rayleigh numbers (Ra) are defined via Eq. (12) [18]:

$$\left.\begin{aligned} Gr_d &= \frac{g\,\beta\,K\,q_w d^2}{\varepsilon\, k_{eff}\left(\frac{\mu_f}{\rho_f}\right)^2}\\ Ra &= Gr_d\times Pr_f \end{aligned}\right\} \quad (12)$$

where

$$\beta = \frac{2}{(T_{in}+T_{out})}$$

Richardson number (Ri) is defined as:

$$Ri = \frac{Gr_{do}}{Re^2} \quad (13)$$

4.Artificial neural network modeling

ANNs are enlivened by the parallel design of a human cerebrum and dependent on the functioning of organic neural systems. They contain a progression of a numerical conditions that are utilized to recreate organic procedures, for example, learning and memory. Normal neurons get motions through neurotransmitters situated on the dendrites, or layer of the neuron. At the point when the receiving signs are sufficient (outperform a specific amount), the neuron is enacted and discharges a prompt through the axon. This prompt may be sent to another neurotransmitter and might energize different neurons [19]. In order to prove the objective of Nusselt number evaluation, the least-squares method is used to solve the problem of the installation of the nonlinear smaller squares curve. This method is also known as Levenberg–Marquardt algorithm (LMA) which was originally proposed in 1944 by Kenneth Levenberg [20] and reclaimed later by Marquardt [21]. This optimization technique combines Gauss-Newton and steepest descent approaches to converge to an optimal solution. Undoubtfully it is one of the effective feedforward neural networks learning algorithm. In addition, it acts gradually as a gradient ratio strategy when the parameters are too far from optimal and are increasingly working like Gauss-Newton when the parameters could be near the optimal solution [22] while avoiding the negative aspects of both techniques. Below the Levenberg Marquart algorithm:

$$[J^T J + \lambda I]\boldsymbol{\delta} = J^T(y - \hat{y}) \quad (14)$$

where J is the Jacobian, λ is the damping parameter, I is the identity matrix, and $\boldsymbol{\delta}$ is increment to estimated parameter vector $\hat{y}$. Adding Fletcher's modification to the aforementioned equation by substituting the identity matrix **I** with the diagonal matrix:

$$[J^T J + \lambda\, diag(J^T J)]\boldsymbol{\delta} = J^T(y - \hat{y}) \quad (15)$$

In this study, the dataset consists of experimental data pairs (N) of an independent of average Nusselt number (Nu), and dependent variables of Prandtl number (Pr), axial distance (x), cylinder angle of inclination (θ),and heat flux(q). In ANN configurations, a two-layer frontal feeding network is represented with a hidden neurons and neurons with linear output in Figure 2. Consequently, to assess the legitimacy of the model, 320 randomized trial data were randomly assigned for training, verification and testing by 70%, 15% and 15%, respectively. Moreover, the trained network with Levenberg-Marquardt backpropagation algorithm created the fitting network. Ultimately, using atrial-and-error method, were three hidden neurons determined gain the optimal model performance and the least error rate.

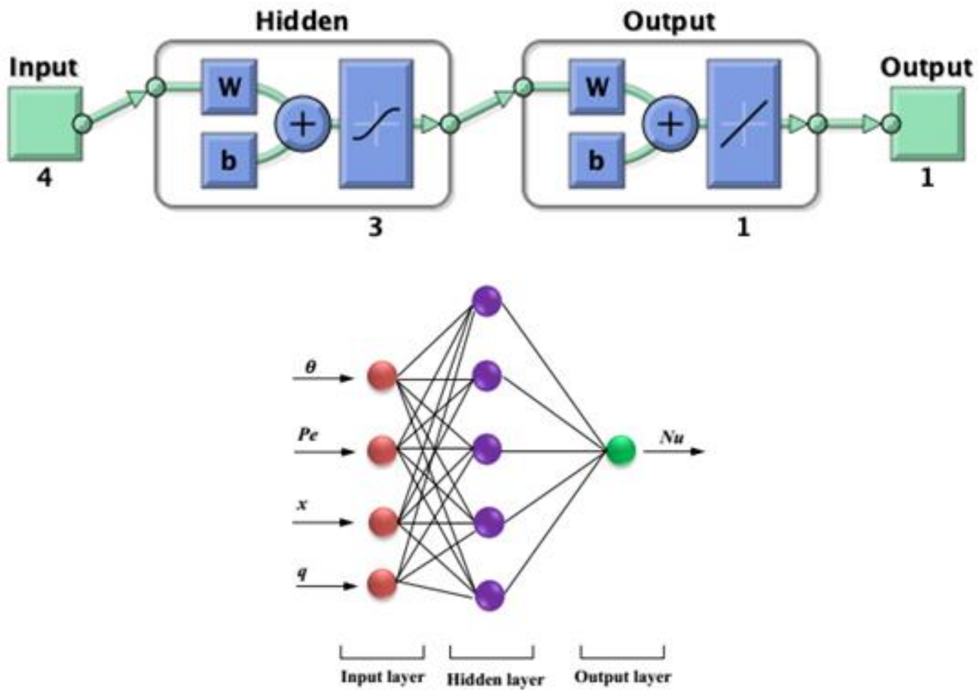

Fig. 2. Schematic of system models [13].

5.Result and Discussion

Fig.3 shows the effect of Pe number on the Nu number for the various inclined angles at a position of 50 mm and constant heat flow of 2160 W /m^2. In general, it is clear from this figure that the average Nussult number increases with the increase of Peclet number in all the inclined angles. It can be seen that the largest Nusselt number is obtained at an inclination angle of 45^o and its behavior corresponding to the Peclet number is different compared to the other cases, the result of the 45^o angle, observed that the average number of Nusselt is not affected by the Peclet number as occurs in other angles. On another side, the distribution of the local Nusselt number has been examined along the tube for constant heat flux (2160 W/m^2 and change Peclet number from (30.3, 172, and 510) as shown in Figs. 4 to 6. From all these figures, it is clear that the local Nusselt number is increased along the tube length in the condition of angle 45^o, while in the other conditions, the local Nusselt number behaving inversely to the tube length on the first half-length of the tube, because of thermal fully developed. As the length progresses, the average number of Nusselt increases rapidly. also, it was seen that the of local Nusselt number in the case of 45^o is higher than other inclined angles and it was not affected by the change in Peclet number for the same heat flux quantity, while in other inclined angles, the local Nusselt number increases with the Peclet number increasing, though the heat flux was constant. The results were compared with a similar study [18]; there was a good match between them. Where n is the number of data points, $Y_i$represents the observed values, and $\hat{Y}_i$represents the predicted values.

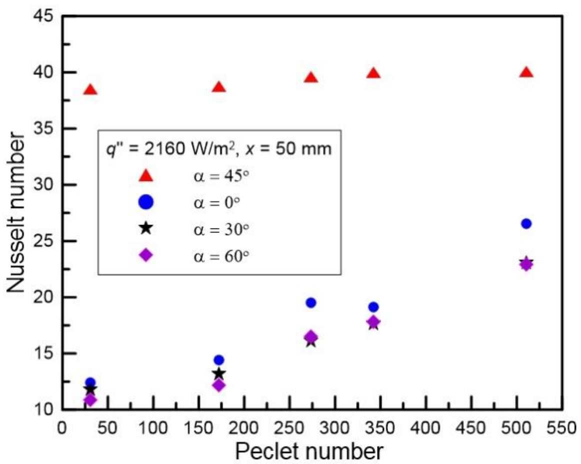

Fig.3. The effect of Peclet number on Nusselt number different angles with $q'' = 2160\ \mathrm{W/m^2}$ and the *x* = 50mm.

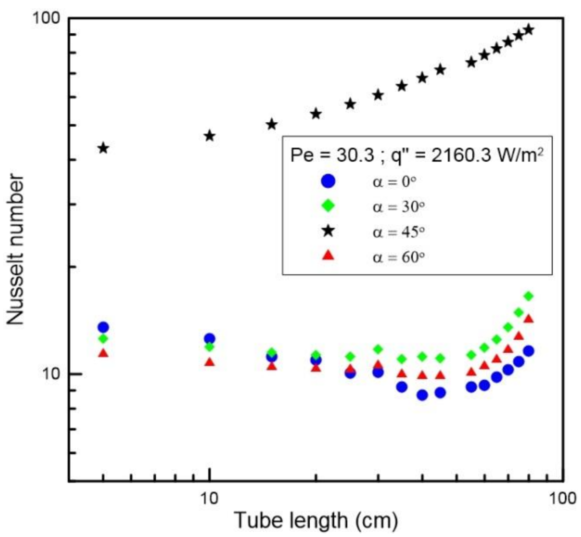

Fig. 4. The distribution of Nusselt number with tube length for *Pe* = 30.3 and $q'' = 2160\ \mathrm{W/m^2}$

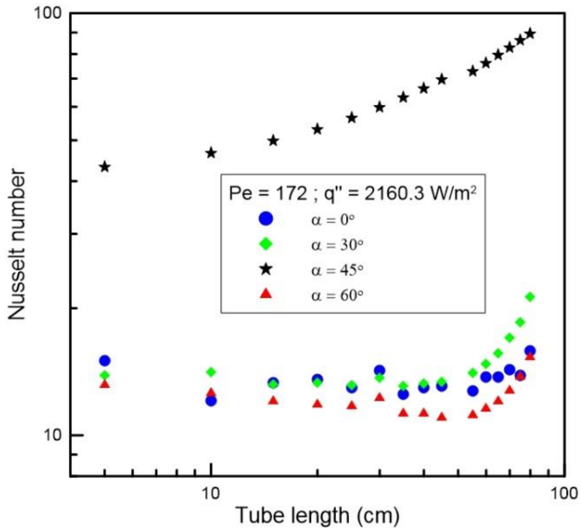

Fig.5. The distribution of Nusselt number with tube length for *Pe* = 172 and $q'' = 2160\ \mathrm{W/m^2}$

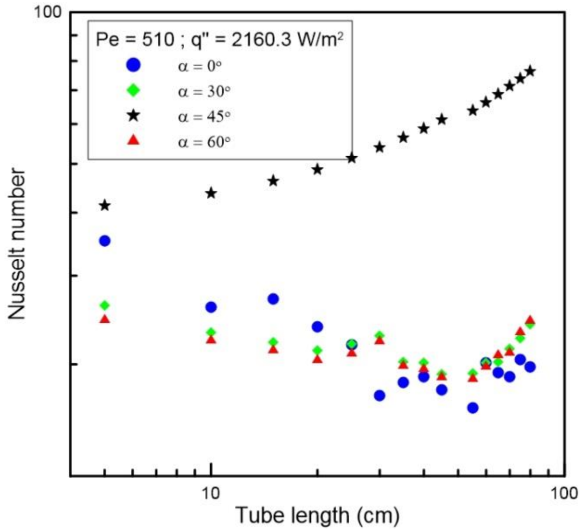

Fig.6. The distribution of Nusselt number with tube length for *Pe* = 510, and $q'' = 2160\ \mathrm{W/m^2}$

The relative error and the mean relative error were respectively defined for each expected output by:

$$RE\% = \frac{|X_{Num} - X_{Pre}|}{X_{Num}} \times 100 \qquad (16)$$

$$MRE\% = \frac{1}{N}\sum_{i=q}^{N}(RE\%)_i \qquad (17)$$

where Num, Pre, and N are referring to the mean numerical values, expected values, and numeric data, respectively. To quantify the degree of the linear correlation between the observed and the predicted values the coefficient of determination is used. The general form for the determination coefficient (R^2) equation is:

$$R^2 \equiv 1 - \frac{SS_{res}}{SS_{tot}} \qquad (18)$$

where SS_{res} is squares sum of the residuals, and SS_{tot} is the total sum of the squares.

The mean squared error (MSE) is a risk function measure the average squared differences between the outputs and targets. Furthermore, it describes the proportion of the nature of an estimator. It is dependably non-negative and approaching closer to zero values are desirable. It is computed as:

$$MSE = \frac{1}{n}\sum_{i=1}^{N}\left(Y_i - \hat{Y}_i\right)^2 \qquad (19)$$

The ANNs model for training data and average Nusselt number shown in Figs. 3 and 4. Where Fig.7 shows the compared between the experimental data with predicted date form ANNs model and Fig. 4 shows the relative error between the real data (experimental) and predicted data. It has been observed that to obtain a better AN gain order in this study, the average relative error is approximately 7.913%. The value of correlation coefficient (R^2) about 99.18%, this value is best.

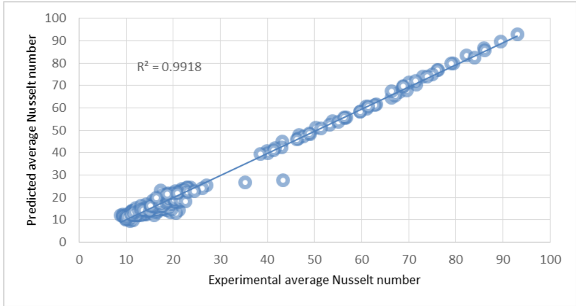

Fig.7. Predictions and Experimental of average Nu by ANNs with Training data.

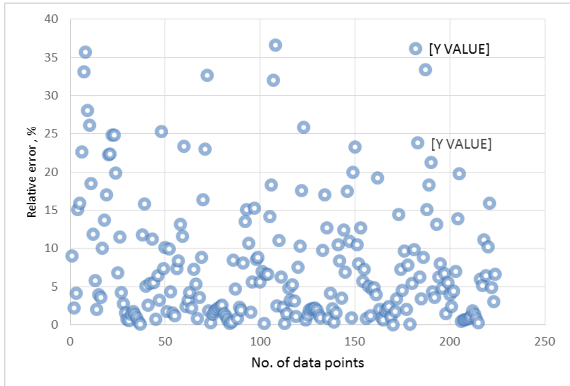

Fig. 8. The relative error of the ANNs model for training data

Once, it was spotted from Figs. 9 and 10 for the testing data for the average Nusselt number. For best order for ANN and average Nusselt number, the mean relative error is 6.641%.and the coefficient of the equation, R-square is 99.46%, where it gives the best agreement between the experimental predictions data and ANNs. These results indicate that the ANNs model is suitable for predicting the heat transfer coefficient in the flow of the porous media channel.

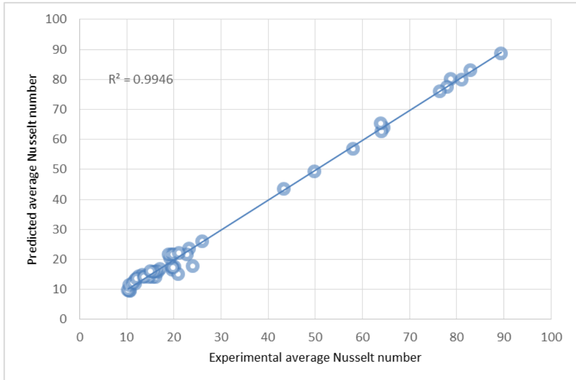

Fig.9. Predictions and Experimental of average Nu by ANNs with testing data.

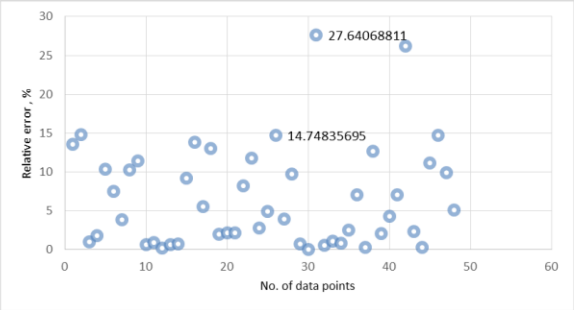

Fig. 10. The relative error of the ANNs model for testing data.

6.Conclusions

This paper includes a detailed experimental study on a mixed convection in circular horizontal tube and inclined with fitted porous media. The second part develop is the ANN model using the Nusselt number was estimated in this system. The ANN model has been shown to be used effectively to estimate heat transfer coefficient in airflow. The results of the study can be summarized as follows:

- Peclet number has a limited effect on average Nusselt and local numbers in case 45. Average Nusselt number was about 2, when Peclet number is changed from 30.3 to 510 for the heat flux 2160 W/m^2, but the other slanted angle conditions were affected significantly by changing Peclet number.
- For the training data, the mean relative error about 7.913% and the R2 is 99.18%.
- For the testing data, the mean relative error about 6.641% and the R^2 is 99.46%.
- Predicting the heat transfer coefficient with the ANN model gives a good compatibility with experimental value and has a lower error. Also, it is present that ANN is more credible for the modeling of such nonlinear systems.

References

[1] Nield DA, Bejan A. Convection in porous media. 2nd Ed., Springer; USA. 1999.
[2] Al-Daher MA. Heat transfer by mixed convection through the horizontal circular tube filled with porous media. Ph.D. Thesis, University of Technology 2000; Baghdad, Iraq.
[3] Pu WL, Cheng P, Zhao TS. An experimental study of mixed convection heat transfers in vertical packed channels. ALAA Journal of Thermophysics and Heat Transfer 1999; 13(4): 517-521.
[4] Dhaher MA, Al-Musawy MH, Al-Samaray AT. An experimental study on forced convection heat transfer an embedded horizontal cylinders array in a porous medium cross flow. Tikrit Journal of Engineering Sciences 2007, 14(1), 1-31.
[5] Manchanda M, Gangawane KM. Mixed convection in a two-sided lid-driven cavity containing heated triangular block for non-Newtonian power-law fluids. International Journal of Mechanical Sciences 2018; **144**: 235-248.
[6] Saeid NH. Analysis of mixed convection in a vertical porous layer using non-equilibrium model. *International Journal of Heat and Mass Transfer*2004; **47**: 5619-5627.
[7] Mohammed HA, Salman, YK. Experimental investigation of mixed convection heat transfers for thermally developing flow in a horizontal circular cylinder. Applied Thermal Engineering 2007; **27**(8), 1522-1533.
[8] Tahseen TA. An experimental study for mixed convection through a circular tube filled with porous media and horizontal an inclined. Modern Applied Science 2011; **5**(2): 128-142.
[9] Mohammed, H.A., Laminar mixed convection heat transfers in a vertical circular tube under buoyancy-assisted and opposed flows. Energy Conversion and Management 2008; **49**(8): 2006-2015.
[10] Tian C, Wang J, Cao X, Yan C, Ala AA. Experimental study on mixed convection in an asymmetrically heated, inclined, narrow, rectangular channel. *International Journal of Heat and Mass Transfer*, 2018; 116: 1074-1084.
[11] Ermis, K., Erek, A.,and Dincer, I. Heat transfer analysis of phase change process in a finned-tube thermal energy storage system using an artificial neural network. International Journal of Heat and Mass Transfer 2007; **50**(15-16): 3163-3175.
[12] Fadare DA, Fatona AS. Artificial neural network modeling of heat transfer in a staggered cross-flow tube-type heat exchanger. The Pacific Journal of Science and Technology 2008;**9**(2): 317-323.
[13] Islamoglu Y, Kurt A. Heat transfer analysis using ANNs with experimental data for air flowing in corrugated channels. *International Journal of Heat and Mass Transfer* 2004; **47**(6–7): 1361-1365.
[14] Genel K, Ozbek I, Kurt A. and Bindal, C. Boriding response of aisi W1 steel and use of artificial neural network for prediction of borided layer properties. Surface and Coatings Technology 2002;**160**(1): 38-43.
[15] Lin TY, Tseng CH. Optimum design for artificial neural networks: An example in a bicycle derailleur system. Engineering Applications of Artificial Intelligence 2000;**13**(1): 3-14.
[16] Tahseen TA, Rahman MM, Ishak M. Experimental study on heat transfer and friction factor in laminar forced convection over flat tube in channel flow. Procedia Engineering 2015; 105: 46-55.
[17] Buonomo BG, Foglia OG, Manca, Nardini S. Numerical study on mixed convection a channel with an open cavity filled with porous media. 5th European Thermal- Sciences Conference 2008; 21-29.
[18] Choi, C. Y. and Kulacki, F.A. Mixed convection through vertical porous annuli locally heated from the inner cylinder. *Journal of Heat Mass Transfer* 1992; 11:143- 151.
[19] Bajpai S., Jain K, Jain N. Artificial neural networks. International Journal of Soft Computing and Engineering 2011: 1: 27–31.
[20] Donald M. An algorithm for least-squares estimation of nonlinear parameters. SIAM Journal on Applied Mathematics 1963;**11**(2): 431–441
[21] Marquardt, An algorithm for least-squares estimation of nonlinear parameters, SIAMJ. Applied Mathematics1963; 11(2): 431441.
[22] Gavin H. The Levenberg-Marquardt method for nonlinear least squares curve-fitting problems. Department of Civil and Environmental Engineering, Duke University (2011): 1-15.